Carbohydrate Polymers 92 (2013) 48–56

Contents lists available at SciVerse ScienceDirect

Carbohydrate Polymers

journal homepage: www.elsevier.com/locate/carbpol

Chitosan/polyethylene glycol fumarate blend film: Physical and antibacterial properties

Azadehsadat Hashemi Doulabi[a], Hamid Mirzadeh[a,*], Mohammad Imani[b], Nasrin Samadi[c]

[a] Department of Polymer Engineering, Amirkabir University of Technology, P.O. Box 15875/4413, Tehran, Iran
[b] Department of Novel Drug Delivery Systems, Iran Polymer and Petrochemical Institute, P.O. Box 14965/115, Tehran, Iran
[c] Department of Drug and Food Control, Faculty of Pharmacy and Biotechnology Research Center, Tehran University of Medical Sciences, P.O. Box 14155/6451, Tehran, Iran

ARTICLE INFO

Article history:
Received 12 August 2012
Received in revised form 2 September 2012
Accepted 3 September 2012
Available online 7 September 2012

Keywords:
Chitosan
Polyester
Film
Blending
Wound dressing

ABSTRACT

The objective of this work was to prepare chitosan/polyethylene glycol fumarate (chitosan/PEGF) blend films as wound dressings and to evaluate the influence of composition ratio on the blending properties of the films. Blending chitosan with PEGF obviated the brittleness of neat chitosan film. Film topography performed by atomic force microscopy illustrated that blending could increase and control the surface roughness of the neat film. Their water vapor transmission rates were close to the range of 904–1447 g^{-2} day^{-1} found to be proper candidates for dressing the wounds with moderate exudates. Controlled water solubility, swelling, wettability and surface tension of the blend films were also evaluated. The blend films showed a powerful antibacterial activity against *Pseudomonas aeruginosa* and *Staphylococcus aureus* (Kill% > 99.76 ± 0.16%). Physical properties as well as antibacterial activity assessments showed that among different compositions, the film comprising 80 wt% chitosan and 20 wt% PEGF is a suitable candidate for biomedical applications as a wound dressing material.

1. Introduction

Recently, there is an increasing interest in the development of wound dressing based on biopolymers as they are biocompatible, biodegradable, and renewable (Boateng, Matthews, Stevens, & Eccleston, 2008). An ideal wound dressing should maintain a moist milieu, absorb excess exudates, allow gaseous exchange, be easy to apply and remove without causing new trauma as well as being antimicrobial, nontoxic and biocompatible (Elsner, Shefy-Peleg, & Zilberman, 2010). Considering exudates discharge and injury location, each type of wound requires specific dressing; hence, the physicochemical and mechanical properties of the dressing should be adjusted (Elsner et al., 2010). Different wound dressings are available commercially in the market, but some of them cannot effectively prevent subsequent microbial outbreak (Seyednejad, Imani, Jamieson, & Seifalian, 2007). Some wound dressings with antibacterial activity make benefit from Ag ion release (Krishna Rao, Ramasubba Reddy, Lee, & Kim, 2012), causing argyria as well as toxicity from the salt or complexes of Ag (Demling & DeSanti, 2001), and the other are based on the releasing of antibacterial agents. There have been noted some side effects for the latter such as microbial resistance due to chronic application of antibacterials and consequent health problems (Atiyeh, Costagliola, Hayek, & Dibo, 2007).

Chitosan, isolated from chitin, is the linear and partly acetylated (1–4)-2-amino-2-deoxy-β-D-glucan (Muzzarelli, 1977, 2012), a well known functional aid for the ordered regeneration of human tissues (Hirano & El-Gewely, 1996; Muzzarelli, Greco, Busilacchi, Sollazzo, & Gigante, 2012). Chitosan is biodegradable, biocompatible, non-antigenic, nontoxic, biofunctional and antimicrobial (Kim, 2011). Chitosan has recently received great attention for different biomedical applications due to its beneficial intrinsic properties. Using intrinsic antibacterial activity of chitosan for wound dressing applications seems promising (Wang, Zhu, Xue, & Wu, 2012) however, chitosan suffers from a relatively poor mechanical characteristic, mainly involving less flexibility resulted in their brittleness at room temperature. There are many reports on blending of chitosan with natural polymers such as konjac glucomannan (Ye, Kennedy, Li, & Xie, 2006), zein (Torres-Giner, Ocio, & Lagaron, 2009), curdlan (Sun et al., 2011) and with synthetic polymers such as poly(ethylene oxide) (Zivanovic, Li, Davidson, & Kit, 2007), poly(vinyl alcohol) (Yang, Su, Leu, & Yang, 2004), poly(vinyl pyrrolidone) (Zeng, Fang, & Xu, 2004), poly(lactic acid) (Suyatma, Copinet, Tighzert, & Coma, 2004) to improve chitosan properties. Several blends, based on chitosan, have also been reported for biomedical applications such as bone (Malafaya & Reis, 2009), cartilage (Alves

* Corresponding author at: Department of Polymer Engineering, Amirkabir University of Technology (Tehran Polytechnic), Hafez Ave., P.O. Box 15875-4413, Tehran, Iran. Tel.: +98 21 64542420; fax: +98 21 66492877.
E-mail address: Mirzadeh@aut.ac.ir (H. Mirzadeh).

0144-8617/$ – see front matter © 2012 Elsevier Ltd. All rights reserved.
http://dx.doi.org/10.1016/j.carbpol.2012.09.002

da Silva et al., 2010), skin (Azad, Sermsintham, Chandrkrachang, & Stevens, 2004) and nerve (Haipeng et al., 2000) tissue engineering as well as drug delivery (Wang, Dong, Du, & Kennedy, 2007).

Usually, polymer blends, rather than single ones, are designed to achieve performances of their constituting ingredients synergistically (Boateng et al., 2008). Blending of two or more polymers has gradually become an important approach to develop new biomaterials exhibiting combinations of properties that could not be achieved by applying each individual polymer (Chen, Wang, Mao, Liao, & Hsieh, 2008). Blends made of both synthetic and natural polymers can provide the wide range of physicochemical properties and processing techniques of synthetic polymers as well as the biocompatibility and biological interactions of natural polymers (Sarasam & Madihally, 2005). To this end, chitosan has been selectively blended with poly(ε-caprolactone) (García Cruz et al., 2008), a biodegradable aliphatic polyester, to obtain desirable mechanical properties.

Fumarate-functionalized unsaturated aliphatic polyesters with tunable mechanical properties have been synthesized as biodegradable materials including polypropylene fumarate (Suggs, Payne, Yaszemski, Alemany, & Mikos, 1997), poly ethylene glycol fumarate (PEGF) (Hashemi Doulabi, Mirzadeh, et al., 2008; Hashemi Doulabi, Sharifi, Imani, & Mirzadeh, 2008), poly(ε-caprolactone) fumarate (Sharifi et al., 2008), polyhexamethylene carbonate fumarate (Sharifi et al., 2011). They have been used as bone cements and substitutes (Holland, Bodde, et al., 2005), cartilage scaffolds (Holland, Tabata, & Mikos, 2005) and drug delivery carriers (Sharifi et al., 2009) but not for wound dressing to the best of our knowledge. PEGF is a biocompatible, cytocompatible, biodegradable member of unsaturated polyesters (Hashemi Doulabi, Mirzadeh, et al., 2008; Shin, Temenoff, & Mikos, 2003) but its weak film forming properties limits its application as a wound dressing material.

For obviating the previously mentioned problems with using neat chitosan and PEGF for wound dressing applications and improving PEGF biological properties, blending of PEGF with chitosan was examined here. It may be an approach to develop new biomaterials exhibiting a combination of properties that could not be obtained by individual ones, *i.e.*, also improved film formation, mechanical properties, tunable water vapor transmission rate, wettability, and ductility of the films.

The objective of the present work was to assess the blend characteristics and evaluate them as wound dressing materials comprising of chitosan and PEGF. This article is dealing with the antibacterial activities of the prepared films to be suitable as a wound dressing. To the best of our knowledge, there is no report in the literature to discuss about chitosan and PEGF blending and the blend properties as a potential biocomposite for wound dressing applications.

2. Experimental

2.1. Materials

Low viscosity chitosan (20–200 mPa s, DDA = 80%, Fluka, Germany) was purified as reported elsewhere (Hashemi Doulabi, Mirzadeh, & Imani, in press). PEG diols (M_w = 3 kDa), calcium hydride, fumaryl chloride, and propylene oxide were all purchased from Aldrich (Milwaukee, MN, USA). Sodium hydroxide, methylene chloride, and acetic acid were obtained from Merck Chemicals (Dusseldorf, Germany). Fumaryl chloride was purified by distillation at 161 °C under ambient pressure. Anhydrous methylene chloride was obtained by distillation under reflux condition for 1 h in the presence of calcium hydride. All of the other chemicals and reagents were of analytical grade and used as received without further purification.

2.2. Methods

2.2.1. Film preparation

PEGF macromer (M_n and $M_w \cong 10$ kDa and 12.2 kDa, respectively, as determined by GPC) was synthesized by esterification of fumaryl chloride with PEG diol in the presence of propylene oxide as a catalyst and proton scavenger, as described in detail elsewhere (Hashemi Doulabi, Mirzadeh, et al., 2008). Chitosan/PEGF blends were prepared by solution casting of polymer solutions in different chitosan/PEGF ratios (0/100, 20/80, 40/60, 60/40, 80/20, 100/0) both dissolved in 1% (v/v) acetic acid. The total concentration of the polymer blends was set on 1 g dL^{-1} for all of the samples composition. After filtration through a syringe filter (Jet Biofil®, 0.45 μm, China), 10 mL of the solution was cast into polystyrene petri dishes ($D \approx 5$ cm). The mixture was left to get completely dried at room temperature then dried *in vacuo* for 48 h. Samples were stored in a refrigerated desiccator until used.

2.2.2. Scanning electron microscopy

Blend films were examined using a T-Scan (Vega II, Czech Republic) scanning electron microscope (SEM). All specimens were coated with a conductive layer of sputtered gold. The micrographs were taken at an accelerating voltage of 15 kV in secondary electron mode to ensure a suitable image resolution.

2.2.3. Swelling behaviors

The fluid absorbing efficiency of a wound dressing is a key design criterion for providing and maintaining a moist environment over the wound bed. It was determined with a gravimetric method. The samples (n = 3) were cut into 1 cm × 1 cm rectangles then dried *in vacuo* (T = 35 °C, P = 0.2 bar) for 24 h and weighted (W_0). Afterward, the samples were immersed in an excess amount of PBS (0.1 M, pH = 7.4) at 25 °C for 24 h. They weighted 10 times at 1 h intervals after removing the water from the surface with blotting paper (W_t). The water uptake (W_u%) was calculated using the Eq. (1):

$$W_u \ (\%) = \frac{(W_t - W_0)}{W_0} \times 100 \quad (1)$$

Water uptake of the blend films at equilibrium condition (EW_u) was obtained using Eq. (1) where the value of the W_t was substituted by the sample weight after 24 h.

2.2.4. Water solubility

The dried films were immersed in methanol, as a non-solvent, for 24 h to remove any residual acetic acid. Then, the samples were taken out and dried *in vacuo* (T = 35 °C, P = 0.2 bar) overnight and weighed (W_1). Afterward, the films (n = 3) were immersed in distilled water for 24 h, dried *in vacuo* overnight, then weighed again (W_2). Water solubility (W_s) was calculated using Eq. (2).

$$W_s \ (\%) = \frac{(W_1 - W_2)}{W_1} \times 100 \quad (2)$$

2.2.5. Water vapor transmission rate

Water vapor transmission rate (*WVTR*) of the sample films was determined according to ASTM E96/E96M-10 (ASTM, 2010) procedure with minor modifications. A glass bottle containing anhydrous silica gel desiccant was covered by the films under test (15 mm diameter in exchange area) and sealed using paraffin wax. The assembly was weighed 8 times at 1 h intervals and kept in a humidity chamber maintaining 75 ± 3% of relative humidity (T = 25 ± 1 °C) using standard saturated solution of sodium chloride. Weight variations of the bottles were plotted *versus* time. *WVTR* was determined

from the slope of this plot obtained by fitting a linear function according to Eq. (3) as below:

$$WVTR = \frac{\text{slop} \times 24}{S}\left[\frac{\text{g}}{\text{m}^2\ \text{day}}\right] \quad (3)$$

where S is the vapor exchange area under test. Control cups, without the anhydrous silica gel desiccant, were conducted in parallel. *WVTR* experiment was repeated thrice for each formulation.

2.2.6. Wettability and surface tension

The static contact angles and surface energies of chitosan and different compositions of chitosan/PEGF blend films were measured using a contact angle goniometer (Sessile Drop, KRUSS G10, Germany). The liquid drops (deionized distilled water or diiodomethane) were separately added onto the surface of the films by a motor-driven syringe at ambient temperature. The data were reported as average of at least three readings. Polarity of the surface and its tension were calculated using Kaelble's equation (Eq. (4)) (Chan, 1994):

$$\gamma_L(1+\cos\ \theta) = 2\sqrt{\gamma_L^d\gamma_S^d} + 2\sqrt{\gamma_L^p\gamma_S^p} \quad (4)$$

where θ stands for the contact angle between solid film and liquid drop, γ_L is surface tension of the liquids (water and diiodomethane) and γ^d and γ^p are the dispersive and polar components of surface tension of the solid and the liquid (subscripts S and L, respectively).

2.2.7. Mechanical properties

Mechanical properties were determined using a SANTAM, STM-20 (Tehran, Iran) universal testing machine. Tensile strength (T_S) and elongation at break (%ε) were determined according to ASTM D882-09 (ASTM, 2009) procedure. A double clamp at a crosshead speed of 1 mm s^{-1} with 20 mm as initial grip separation was used. T_S was calculated by dividing the maximum load by the cross-sectional area and %ε was determined by dividing the extension at break by the initial gauge length of the films and multiplying by 100. Elastic modulus (E) can be experimentally determined from the slope of a stress–strain curve.

2.2.8. Analysis of surface topography

Surface analysis of the films was done by atomic force microscopy (AFM) (DualScope™ 95-200, Denmark) at ambient conditions. Sample films were attached onto iron AFM substrate disks using double-sided adhesive tape. Topographic images were obtained in none contact mode using silicon microcantilever probes with a tip radius of 15 nm. The probe oscillation resonance frequency was 120 kHz and scan rate was 1 Hz (force: 0.12 nN). Images were captured at different locations, and roughness factors were calculated using the associated software (DME Dual Scope™/Rasterscope (tm) SPM 2.1.1.2). The results were showed as the root mean square surface roughness (S_q) and presented as arithmetical mean height ± standard deviation.

2.2.9. Antibacterial activity assay

Bactericidal activity of the samples was evaluated against *Pseudomonas aeruginosa* ATCC 9027 as a Gram-negative bacterium and *Staphylococcus aureus* ATCC 6538 as a Gram-positive bacterium by determining viable cell counts after exposure with test samples. An overnight culture of each bacterium was used to prepare a bacterial suspension with a cell density approximately equivalent to 10^8 CFU mL^{-1}. The film samples were cut into pieces with 25 mm in diameter, immersed in 70% (v/v) ethanol then washed with sterile PBS solution and air dried under Laminar air flow (LAF) to reduce microbial contamination (Sarasam, Krishnaswamy, & Madihally, 2006). Each film was added into 10 mL nutrient broth medium (Merck, Germany) which was then inoculated with bacterial suspension to reach the final concentration of 10^7 CFU mL^{-1}. After 24 h exposure at room temperature, each sample was serially diluted and the number of survived bacteria was determined by pour plate method using nutrient agar medium (Merck, Germany). The plates were incubated at 37 °C for 48 h and the number of bacteria was reported as the survival population of the test organisms (Yang, Lin, Wu, & Chen, 2003). Eq. (5) was used to calculate the killing efficacy as Kill% (Li et al., 2011). In addition, the population reduction of the test organism was obtained using Eq. (6). As mentioned in the standard method, at least a 1 Log reduction of bacterial load is required to claim antibacterial property (Pinto et al., 2012). Nutrient broth containing the same bacterial inoculum and no film was used as control.

$$\text{Kill\%} = \frac{\text{cell count of control} - \text{cell count of sample}}{\text{cell count of control}} \times 100 \quad (5)$$

$$\text{Log population reduction} = \text{Log cell count of control} - \text{Log survivor count on sample} \quad (6)$$

2.3. Statistical analyses

Analysis of Variance (ANOVA) and linear regression were the main statistical tools used for data analysis. The Tukey ($\alpha = 0.05$, 95% confidence intervals) was also used to determine the significance of differences between specific means (Origin®, 7.0, 2002, USA).

3. Results and discussion

3.1. Preliminary characterization

Chitosan/PEGF blends of varying blend ratios were successfully prepared in this study. According to the preliminary test results, chitosan and its blend films were semi-clear and slightly yellowish in color. Film thickness (average 30–70 μm) was determined using a micrometer (Mitutoyo 156-101, Japan) by performing at least five measurements per sample. Film thickness was significantly increased ($p < 0.05$) by increasing in chitosan content in the blends.

3.2. Morphological examinations

Surface morphology of different chitosan/PEGF blend films was evaluated using SEM micrographs of surface of the films as illustrated in Fig. 1. Microstructures obtained by SEM for the blended films prepared by mixing the polymers solution and consequent solvent casting, showed that PEGF particles were relatively well dispersed in the chitosan matrix. Fig. 1 shows that the blends are homogeneous at low concentration of PEGF in the blends composition *i.e.*, 20, 40 and 60% (w/w) implying partial miscibility of the components. As concentration of the PEGF component was increased from 60 to 80% (w/w); the surface homogeneity of the films was decreased to some extent, with phase separation; however, phase separation between chitosan and PEGF in the blend films could not be completely detected by electron microscopy. The chitosan film morphology in Fig. 1(e) shows featureless film matrix with smooth surfaces. Surfaces of the blend films were rougher than the chitosan film, as shown in Fig. 1. This finding was supported by AFM observations. Pores were not observed on the surface of the chitosan and its blend films in contrast to Baimark and Srihanam (2010). As mentioned before, homogeneous and uniform dispersion of chitosan is shown in Fig. 1(a).

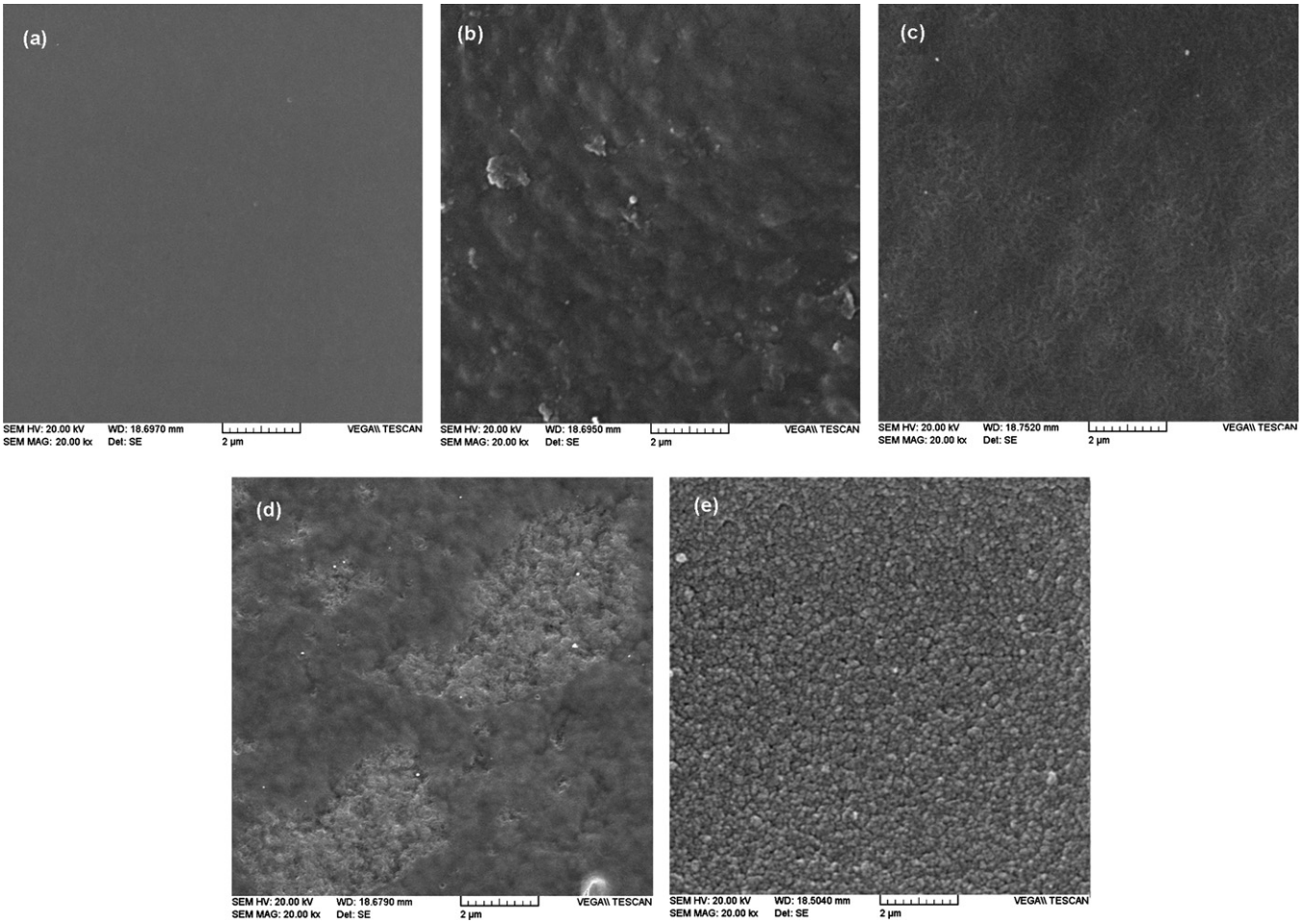

Fig. 1. SEM micrographs of chitosan/PEGF blend films surface in different compositions consisting of 100/0 (a), 80/20 (b), 60/40 (c), 40/60 (d), 20/80 (e) samples.

3.3. Swelling study

The swelling behavior of the films were investigated and reported as equilibrium water uptake (EW_u%) in Fig. 2. The values of EW_u showed that all films had water retention capability and EW_u of the blend films could be correlated to the chitosan/PEGF blend ratios as well as physical structure of the blend films. In other words, the blends with 80/20 and 60/40 in chitosan/PEGF ratio yielded the higher EW_u% than 100/0 and 40/60 blend ratios. The increment of PEGF content in the blend films after the blend ratio variation resulted in increasing EW_u% values from 122% in neat chitosan to 258% and 305% for the blends with 80/20 and 60/40 ratios, respectively. This could be attributed to the increasing presence of hydrophilic groups (—OH) in the blends. In our case, the blend with ratio 40/60 showed reduced W_u. However the hydrophilic content was high but the interactions between the functional groups of chitosan and PEGF should not be ignored.

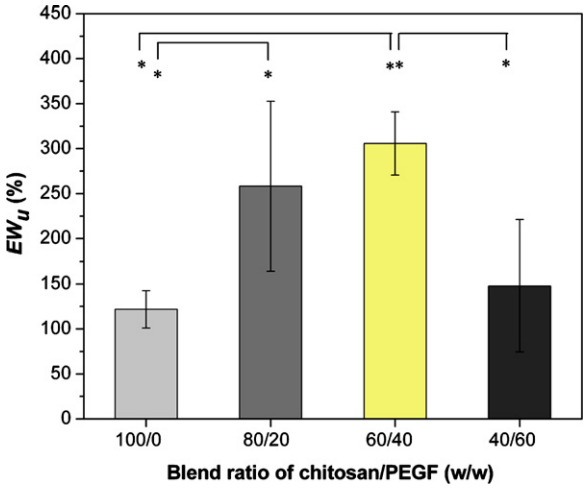

Fig. 2. Equilibrium water uptake (EW_u) of chitosan/PEGF films for different blend ratios, bar graphs show $^*p < 0.05$.

To evaluate the capacity of the chitosan/PEGF blend films to absorb exudates, dynamic water uptake (W_u) study against time was also assessed in PBS solution (pH = 7.4) and the results are depicted in Fig. 3. All films swelled rapidly in a short period of time (*ca.* 10 min) and reached equilibrium within approximately 6 h and the capacity of water uptake declined because of the presence of PEGF. Due to the poor film formation properties of 20/80 and 0/100 chitosan/PEGF compositions no result was provided for these samples. In fact, swelling of the PEGF containing blend films occurred simultaneously with their degradation in PBS medium due to leaching of PEGF from films during time however, these two phenomena got balanced finally at some period of time. At the beginning of swelling studies, W_u predominated over degradation. At the same time, the compact structure of the blend films were broken down gradually and filled with water promoting the dissolution of PEGF into PBS hence accelerated degradation. While degradation dominated, EW_u values decrease gradually until the blend structures collapsed.

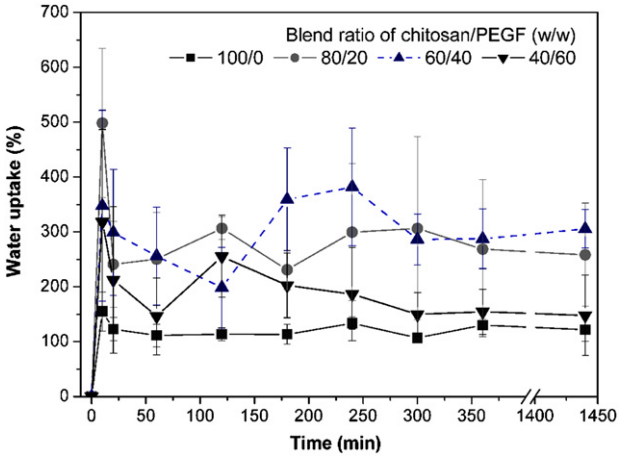

Fig. 3. Water uptake (W_u) study of chitosan/PEGF films for different blend ratios, bar graphs show $^*p < 0.05$.

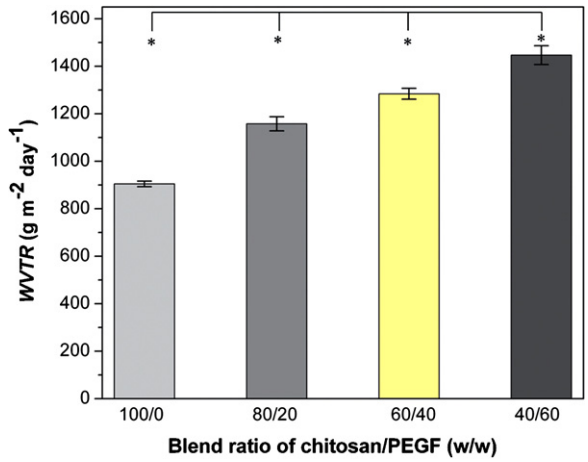

Fig. 5. Effect of blending on *WVTR* for different blend ratios of chitosan/PEGF, bar graphs show $^*p < 0.05$.

3.4. Water solubility

PEGF is a water-soluble polymer while chitosan is insoluble in pure water at neutral pH but certain chitosan salts are promptly soluble in water. It is worthy of note that controlled solubility of biodegradable films offers many potential benefits for use as biomaterial devices therefore the importance of water solubility of the films gets more attention. The results for water solubility of chitosan/PEGF blend films are depicted in Fig. 4. According to the results, water solubility of the blend films increased rapidly with increasing in PEGF content; meanwhile the one for the neat chitosan was $2.11 \pm 0.60\%$. Although all the films kept up the original shape upon water immersion for 24 h at room temperature, but the weight loss of the blend films was increased by decrement of the blend ratios, (*e.g.*, chitosan/PEGF: 40/60 films dissolved in the media the most *i.e.*, $50.22 \pm 9.31\%$). Fig. 4 shows the blend ratios have significant effect on the water solubility ($p < 0.05$). This phenomenon may result in decrement of tensile strength at both wet and dry conditions. Further investigations on mechanical properties at wet condition are in progress.

3.5. Water vapor transmission rate

In order to prevent dehydration and excessive buildup of exudates and control the water loss from a wound at an optimal rate, a wound dressing should conform with essential properties like *WVTR* (Balakrishnan, Mohanty, Umashankar, & Jayakrishnan, 2005). The optimal *WVTR* causes to create an environment with a moisture level ideal for wound healing. The results of the *WVTR* tests for the different chitosan/PEGF blend ratios are shown in Fig. 5. All blends behaved in a similar fashion as that of the water solubility, *i.e.*, by decreasing the blend ratio, thereby increment in PEGF content in the films, more moisture were absorbed from atmosphere into the films. Thus a hydrated film should be able to facilitate vapor transfer from a moisture rich environment to a dry environment. It has been reported that water vapor transmission through a hydrophilic film depends on several factors such as solubility and diffusivity of water molecules in the film (Gontard & Guilbert, 1994). In our case, the interactions of the permeating water molecules with the polar groups in the chitosan film were the important subject needed to be considered. It may be attributed to diffusivity of water molecules through the film. On the other hand, it could be due to the existence or progress in intermolecular interactions between chitosan and PEGF molecules. Of course, there was a strong hypothesis that the miscibility of the blend was decreased by increasing in the polyester content. The lack of total miscibility between the two components of the blend may result in forming some micro domains, rich in PEGF, which enhances moisture penetration through these preferential pathways and consequently increases the *WVTR* value. Lack of total miscibility is previously shown in SEM micrographs (see Fig. 1) and will be confirmed more by mechanical findings reported in the next sections. It has been reported that *WVTR* values for normal skin, first degree burns and granulating wounds are 204 ± 12, 279 ± 26, and $5138 \pm 202\ g\,m^{-2}\,day^{-1}$, respectively (Elsner et al., 2010). The low *WVTR*s of the commercial wound dressings, fabricated as films, lead to the accumulation of exudates, hence; bacterial penetration and growth risks during the healing process will be inevitable. An excessive *WVTR* will lead to total dehydration of the wound surface, causing the wound dressing to adhere to the wound surface. Our results are comparable with commercial wound dressings available in market such as Dermiflex® (J&J), Tegaderm®, Bioclusive® (J&J), Op Site® (J&J), Biobrain®, Lyofoam, Geliperms (Geistlich Ltd.) and Vigilons (Bard Ltd.) having *WVTR*s of 90 ± 3, 491 ± 41, 394 ± 12, 792 ± 32, 1565 ± 51, 3052 ± 684, 9009 ± 319 and $9360 \pm 34\ g\,m^{-2}\,day^{-1}$, respectively (Yoo & Kim, 2008). The prepared films have neither high nor low *WVTR* values. Hence, considering the generally accepted optimal *WVTR* value, the films with *WVTR* close to the range of $904–1447\ g\,m^{-2}\,day^{-1}$ found to be candidates for dressing the wounds with moderate exudates.

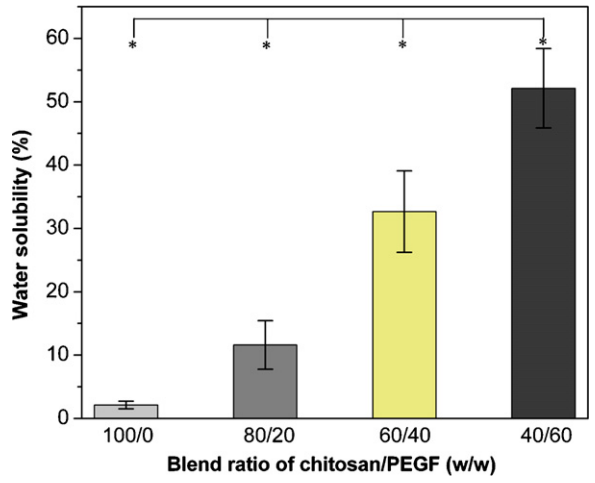

Fig. 4. Effect of blending on water solubility for different blend ratios of chitosan/PEGF, bar graphs show $^*p < 0.05$.

Table 1
Characterization data of contact angle and surface tension of various chitosan/PEGF blends.

Blend ratio of chitosan/PEGF (w/w)	Contact angle (°)		SD%	Surface tension (mN m^{-1})		
	θ_w	θ_d		γ_{Total}	γ_p	γ_d
0/100	60.00	56.40	0.87	42.80	12.20	30.60
40/60	55.80	41.00	2.41	54.53	15.45	39.08
60/40	57.20	34.00	0.34	54.65	13.15	41.51
80/20	59.90	29.10	1.21	55.41	10.81	44.59
100/0	92.10	57.60	3.00	32.01	2.04	29.97

γ_d: London dispersion forces; γ_p: polar (Keesom) forces.

The blend films studied here are potentially capable to maintain a proper fluid balance on the wound bed, which can facilitate cellular migration and enhance reepithelialization.

3.6. Wettability and surface tension

Surface wettability is critical for optimal application of films in biomedical fields as wound dressing materials. A number of indirect empirical and semi-empirical techniques have been developed based on contact angle measurement to measure surface tension of solids. Kaelble's equation (Eq. (4)) is frequently used to determine the polar and dispersive components of polymer surface tensions because of its simplicity. This equation allows the determination of the surface tensions of the polar and dispersive components of a polymer by measuring the contact angles of two liquids of known surface tension on the polymer surface (Chan, 1994). The polar and dispersive components of the surface tension of the blends are listed in Table 1. They were obtained after solving Eq. (4) for two liquids, water and diiodomethane, simultaneously. To examine the hydrophilicity of the blend films, their water contact angles were measured and the results were inserted in Eq. (4). The water contact angles (θ_w) for all films were small *ca.* 55–60° showing that these materials have good hydrophilicity thereby they are suitable for cell supporting (Solouk et al., 2011). Blending chitosan with PEGF could affect the surface wettability. Surface chemical groups were indicated to be one reason causing the surface wettability of the blend films. The contact angle was lowered to some extent by introducing PEGF but it did not changed much or even increased slightly when the chitosan/PEGF proportion was increased from 40/60 to 80/20. The contact angle of chitosan was the largest one which means that the wettability of the chitosan was lower than that of its blends. Therefore, the addition of too much PEGF impaired their surface properties. The enhanced hydrophilicity, caused by the addition of PEGF, can be attributed to PEGF chains positioned on the material surfaces. PEGF has hydrophilic polymer segments *i.e.*, PEG which would improve the wettability when blended, dispersed and randomly placed on the film surface. The obtained results may also partly be attributed to the availability of the terminal hydroxyl groups of PEGF since —OH functional groups may possibly improve the hydrophilicity of biomaterials surface and suggests additional interactions with water molecules that influence the wettability of the films (Zhang, Li, Gong, Zhao, & Zhang, 2002). There is an important point to note that blending may change the surface physics. In our case, the increment of PEGF content in the blends caused a significant decrease in θ_w, which indicates that the topography of the films with different blend ratios could influence the liquid–solid interface.

The most significant difference in surface tension was observed between chitosan, as neat film, and its blends with PEGF. A decrease in the water contact angle values was observed with an increase in PEGF component concentration. As a result, the highest surface tension of 55.41 mN m^{-1} was obtained for 80/20 (chitosan/PEGF blend ratio) samples. A possible explanation for these observations could be short-range interactions such as hydrogen bonding that tie up the polar groups of both blend components together. Usually an increase in the polar component of surface tension is an indication of an increase in the polar groups existing on the surface (Ratner, 1996). Extensive changes in the polar component of the surface tension values from 2.04 to 15.45 mN m^{-1} were observed. There are two possible reasons for this observation. The first is concerning with the short aliphatic chains of PEGF, and the second is the possible interactions and/or chemical bonds between PEGF and chitosan. It should be noted that the wettability could not always be directly correlated to the surface composition (Correlo et al., 2007). Surface composition can vary during the measurements due to the possible interactions between the two phases (water and the blend).

3.7. Mechanical properties

Mechanical properties of wound dressings are important factors affecting their performance. The mechanical properties of the blend films including modulus of elasticity (E), strain at break ($\%\varepsilon$) and tensile strength (T_S) were characterized and compared with the neat chitosan films. Neat chitosan films were brittle with an E of 577.5 MPa and $\%\varepsilon$ of 7.50 ± 0.28%. In fact, these films have high E and T_S but low $\%\varepsilon$ in comparison with the blend films, which can be taken as evidences on film brittleness. The values of Table 2 show the strong reduction in modulus for the blend films. In these blends, the increment of $\%\varepsilon$ with increasing in PEGF content can be regarded as evidence on more elasticity of the samples as a function of more PEGF content. Considering the rigid structure of chitosan, originated from weak but high number of intramolecular bond forces, like H-bonds, *etc.*, introducing PEGF may seriously destroy the crystallinity of chitosan, thereby increases the amorphous phase. In the other words, adding PEGF to the film composition caused it to become ductile. As a consequence, all blends generally showed a decrease in the E, T_S, and $\%\varepsilon$ with the increase in their PEGF contents. However, a different result was observed in the value of E for the blends with 60/40 blend ratio. Unlike to chitosan/PEGF: 80/20, the blend with 60/40 blend ratio showed decrement in tensile strength and elongation at break while increment in initial modules. This finding would be due to the lack of total miscibility. This hypothesis was confirmed by SEM images (see Fig. 1(c)). The 80/20 chitosan to PEGF ratio was an optimum choice in the mechanical properties of the blends since the introduction of PEGF to the chitosan made the films to be more flexible and ductile. This sample possessed both the relatively high T_S and E along with good flexibility ($\%\varepsilon$). It actually demonstrated better mechanical properties than some wound

Table 2
Tensile strength, elongation at break and elastic modulus of chitosan and its blends, data are presented as mean ± SD.

Blend ratio of chitosan/PEGF (w/w)	Tensile strength (MPa)	Elongation at break (%)	Elastic modulus (MPa)
60/40	12.29 ± 5.43	4.10. ± 0.75	401.19 ± 41.40
80/20	91.93 ± 11.21	11.50 ± 0.70	138.31 ± 59.91
100/0	41.53 ± 4.01	7.50 ± 0.28	577.50 ± 40.07

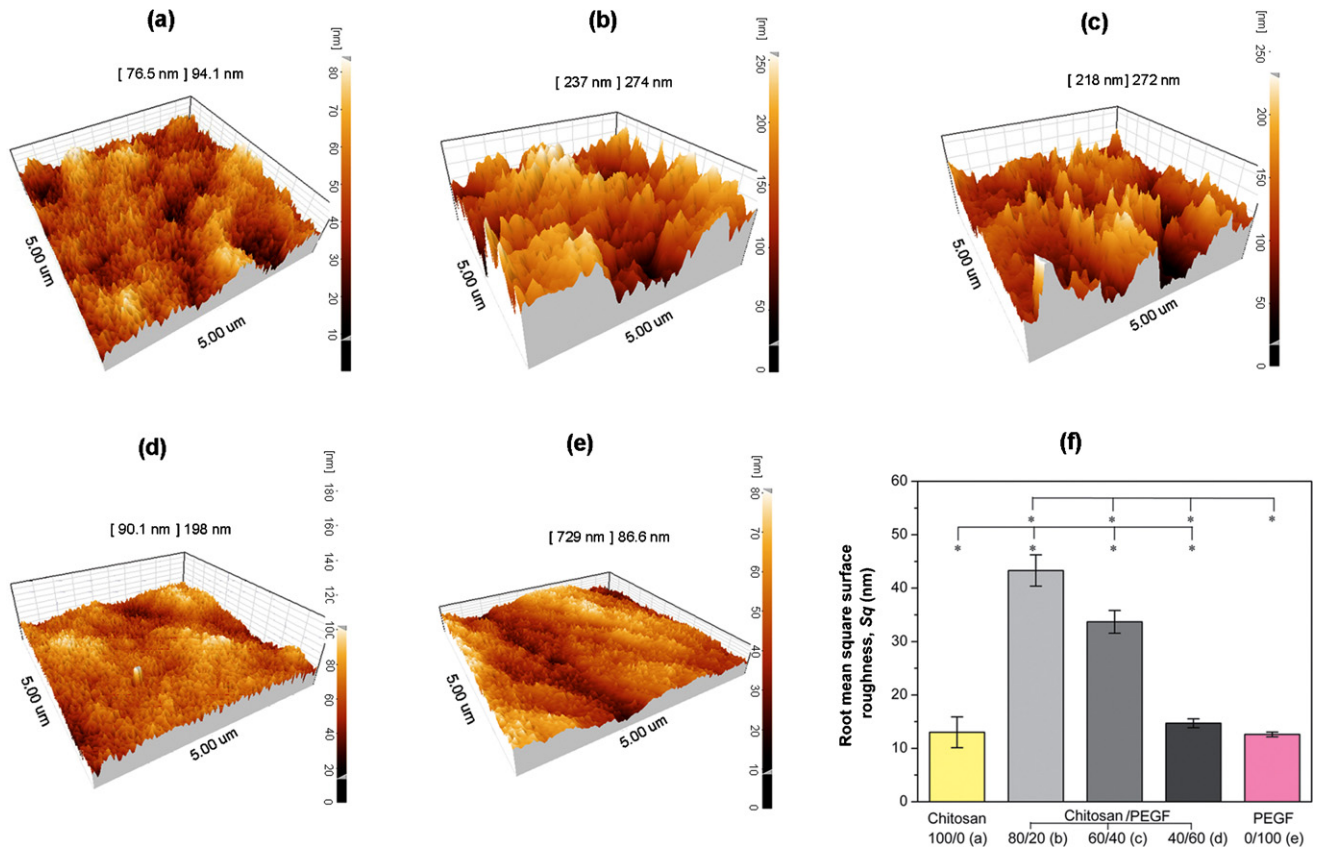

Fig. 6. Effect of blending on surface morphology of different blend ratios of chitosan/PEGF: 100/0 (a), 80/20 (b), 60/40 (c), 40/60 (d), 0/100 (e). The plot of blend ratios *versus* roughness (f), bar graphs show $^{*}p < 0.05$.

dressings currently used or studied, such as Kaltostat® (ConvaTec) with 1.30 ± 0.20 MPa, $0.90 \pm 0.10\%$, and 10.80 ± 0.40 MPa as T_S, $\%\varepsilon$, and E (Chiu, Lee, Chu, Chang, & Wang, 2008). Introducing PEGF to chitosan could obviate the brittleness of chitosan while other essential properties remained untouched as a wound dressing material.

3.8. Analysis of surface topography

Surface morphology of the films was probed using AFM in non-contact mode and three dimensional surface plots were prepared. The topographic images for different blend ratios are depicted in Fig. 6(a)–(e) and the values of the root mean square of roughness are summarized in Fig. 6(f). It is observed in Fig. 6(a) and (e) that neat chitosan and PEGF films have smooth surfaces with uniformly distributed short spikes. Introduction of PEGF to chitosan increased the height of these spikes and a significant increase in S_q from 13.0 to 43.3 nm. The chitosan/PEGF: 80/20 showed the tallest spikes over a large area whereas neat PEGF was smoother than all of the blends. Maximum roughness was observed in the chitosan/PEGF: 80/20 blend, which was significantly higher than chitosan/PEGF: 60/40 and 40/60 samples. Considering morphology of the blended films (resulted from SEM images), it is worthy to note that increment in surface roughness indicated that the polymers were partially compatible but not incompatible.

The effects of blending on the surface characteristics can be elucidated by considering the wettability and topography results together. The relatively higher θ_w values for films with rough surface of each film composition can be attributed to the accumulation of more air pockets on the inter-space than films with smooth surface thereby decrement in hydrophilicity of the blend film. In another word, surface roughness of the films results in air entrapment on the film interfaces which affects θ_w values, in turn. In the neat PEGF samples, the surface chemistry was dominant on surface physics.

3.9. Antibacterial activity

It is known that chitosan is an antibacterial (bacteriostatic and bactericidal) agent to 297 bacterial strains (Muzzarelli et al., 1990). In this study, PEGF is introduced in chitosan films to modify brittleness of chitosan but it is more important to assess if the chitosan/PEGF blends possess antibacterial properties against Gram-positive and Gram-negative bacteria. The results of antibacterial activity tests of chitosan and the blend films as surviving bacteria and population reduction are depicted in Fig. 7(a) and (b) and the values of killing efficacy are shown in Fig. 7(c).

All samples including chitosan and chitosan/PEGF films reduced the number of *P. aeruginosa* as a Gram-negative bacterium and *S. aureus* as a Gram-positive bacterium by approximately 3 Log CFU mL^{-1} comparing to the positive control of 9.79 Log CFU mL^{-1}. The results showed that the films had satisfactory antibacterial properties. All chitosan compositions showed significantly different ($p < 0.05$) antibacterial activity against *P. aeruginosa* except for films 80/20 in comparison with 60/40 chitosan/PEGF. However, in the case of *S. aureus*, the reduction in viable cells on the films of 100/0 in comparison with 80/20 blend ratio (chitosan/PEGF) showed no significant difference ($p > 0.05$).

By increasing content of PEGF (in the blend films with 80/20 to 60/40 in ratios), the distribution of PEGF components on the surface of the films may decrease the possibility of interaction of chitosan with bacteria and reduce lethality of the films but their differences were not significant except for *P. aeruginosa*. It may be due to the concentration of chitosan in the films needed for

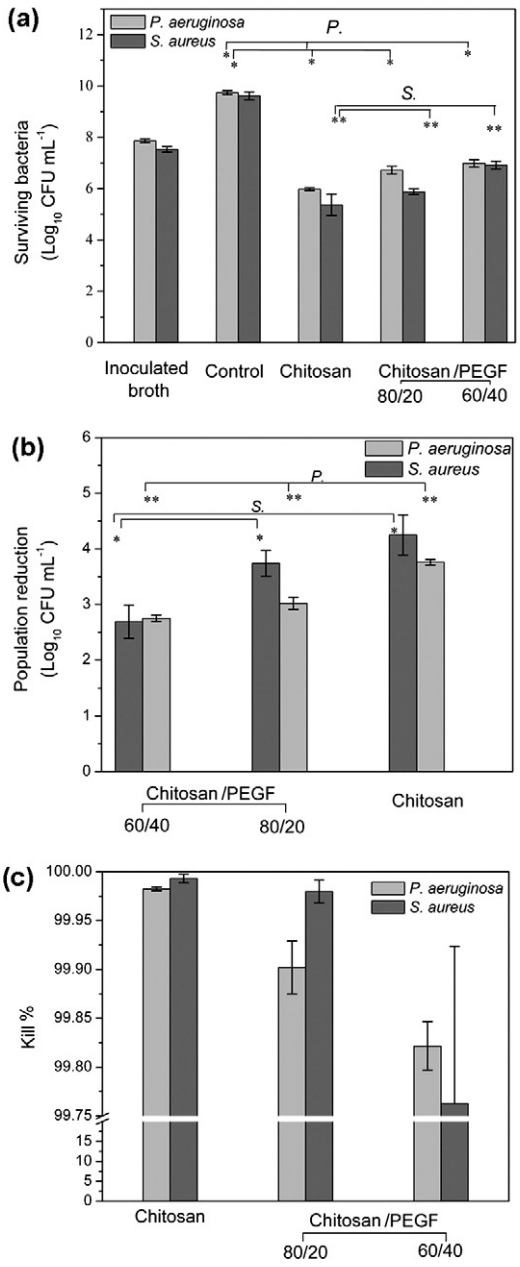

Fig. 7. Survival of two test bacteria (Log_{10} CFU mL^{-1}) after 24 h exposure to 100/0, 80/20 and 60/40 of chitosan/PEGF blend films in comparison with initial inoculated broth, positive control is inoculated broth without film (a). Population reduction of two test bacteria (Log_{10} CFU mL^{-1}) after 24 h exposure to 100/0, 80/20 and 60/40 of chitosan/PEGF blend films (b), bar graphs show * and ** $p < 0.05$. Kill% of 100/0, 80/20 and 60/40 of chitosan/PEGF blends against *P. aeruginosa* and *S. aureus* in nutrient broth (c).

inhibiting the growth of this test strain as well as hydrophilicity of the film surfaces. However surface roughness could be influenced the bacterial adhesion (Chin, Sandham, de Vries, van der Mei, & Busscher, 2007), but the resultant of surface chemistry and surface physics could be a determining factor which affects kill% of bacteria.

The main mechanism for antibacterial activity of chitosan is not completely clear, but different mechanisms have been proposed (Feng & Xia, 2011). Attraction of sections of anionic microbial membrane into the internal pores provided by removing PEGF molecules from the film lead to disruption of anionic phospholipid section in bacterial cell membrane and then microbial death was proposed as the possible mechanism of antimicrobial activity for the blend films. Similar mechanism has been reported elsewhere by Li et al. (2011) for quaternized chitosan hydrogel films.

4. Conclusions

In this study, blend films of chitosan/PEGF with different compositions were prepared which had powerful antibacterial activity against *P. aeruginosa* and *S. aureus*. The relationship between physicochemical characteristics of the blend films and blend ratios was assessed. Decrement in chitosan/PEGF blend ratios resulted in increasing of swelling ratio and *WVTR* of these films. Blending chitosan with PEGF not only improved mechanical properties but also affected the surface roughness and wettability of neat chitosan. The chitosan/PEGF films with 80/20 in blend ratio due to their superiorities including acceptable mechanical strength, good transparency, high water uptake and suitable *WVTR* as well as the antibacterial activity showed this biocomposite is a suitable candidate for biomedical applications as a wound dressing.

Acknowledgments

The authors would like to express their sincere gratitude to Iran National Science Foundation (No. 89001749) and also Department of Drug and Food Control of Tehran University of Medical Sciences for supporting this research.

References

Alves da Silva, M. L., Crawford, A., Mundy, J. M., Correlo, V. M., Sol, P., Bhattacharya, M., et al. (2010). Chitosan/polyester-based scaffolds for cartilage tissue engineering: Assessment of extracellular matrix formation. *Acta Biomaterialia*, *6*, 1149–1157.

ASTM Standards, D882-09. (2009). *Standard test method for tensile properties of thin plastic sheeting*. West Conshohocken, PA: ASTM International. http://dx.doi.org/10.1520/D0882-09, www.astm.org

ASTM Standards, E96/E96M-10. (2010). *Standard test methods for water vapor transmission of materials*. West Conshohocken, PA: ASTM International. http://dx.doi.org/10.1520/E0096_E0096M-10, www.astm.org

Atiyeh, B. S., Costagliola, M., Hayek, S. N., & Dibo, S. A. (2007). Effect of silver on burn wound infection control and healing: Review of the literature. *Burns*, *33*(2), 139–148.

Azad, A. K., Sermsintham, N., Chandrkrachang, S., & Stevens, W. F. (2004). Chitosan membrane as a wound-healing dressing: Characterization and clinical application. *Journal of Biomedical Materials Research Part B: Applied Biomaterials*, *69*, 216–222.

Baimark, Y., & Srihanam, P. (2010). Study on nanostructures of chitosan/poly(ethylene glycol) blend films. *International Journal of Applied Chemistry*, *6*, 247–254.

Balakrishnan, B., Mohanty, M., Umashankar, P. R., & Jayakrishnan, A. (2005). Evaluation of an in situ forming hydrogel wound dressing based on oxidized alginate and gelatin. *Biomaterials*, *26*, 6335–6342.

Boateng, J. S., Matthews, K. H., Stevens, H. N., & Eccleston, G. M. (2008). Wound healing dressings and drug delivery systems: A review. *Journal of Pharmaceutical Sciences*, *97*, 2892–2923.

Chan, C. M. (1994). Contact angle measurement. In *Polymer surface modification and characterization*. Munich Vienna New York: Hanser/Gardner Publications, Inc.

Chen, C. H., Wang, F. Y., Mao, C. F., Liao, W. T., & Hsieh, C. D. (2008). Studies of chitosan. II. Preparation and characterization of chitosan/poly(vinyl alcohol)/gelatin ternary blend films. *International Journal of Biological Macromolecules*, *43*, 37–42.

Chin, M. Y. H., Sandham, A., de Vries, J., van der Mei, H. C., & Busscher, H. J. (2007). Biofilm formation on surface characterized micro-implants for skeletal anchorage in orthodontics. *Biomaterials*, *28*, 2032–2040.

Chiu, C. T., Lee, J. S., Chu, C. S., Chang, Y. P., & Wang, Y. J. (2008). Development of two alginate-based wound dressings. *Journal of Materials Science: Materials in Medicine*, *19*, 2503–2513.

Correlo, V. M., Pinho, E. D., Pashkuleva, I., Bhattacharya, M., Neves, N. M., & Reis, R. L. (2007). Water absorption and degradation characteristics of chitosan-based polyesters and hydroxyapatite composites. *Macromolecular Bioscience*, *7*(3), 354–363.

Demling, R., & DeSanti, L. (2001). Effects of silver on wound management. *Wounds*, *13*, 5–14.

Elsner, J. J., Shefy-Peleg, A., & Zilberman, M. (2010). Novel biodegradable composite wound dressings with controlled release of antibiotics: Microstructure, mechanical and physical properties. *Journal of Biomedical Materials Research Part B: Applied Biomaterials*, *95*, 425–435.

Feng, Y., & Xia, W. (2011). Preparation, characterization and antibacterial activity of water-soluble O-fumaryl-chitosan. *Carbohydrate Polymers*, *83*, 1169–1173.

García Cruz, D. M., Coutinho, D. F., Costa Martinez, E., Mano, J. F., Gómez Ribelles, J. L., & Salmerón Sánchez, M. (2008). Blending polysaccharides with biodegradable polymers. II. Structure and biological response of chitosan/polycaprolactone blends. *Journal of Biomedical Materials Research Part B: Applied Biomaterials*, *87*, 544–554.

Gontard, N., & Guilbert, S. (1994). *Food packaging and preservation*. London: Blackie Academic & Professional.

Haipeng, G., Yinghui, Z., Jianchun, L., Yandao, G., Nanming, Z., & Xiufang, Z. (2000). Studies on nerve cell affinity of chitosan-derived materials. *Journal of Biomedical Materials Research Part A*, *52*, 285–295.

Hashemi Doulabi, A., Mirzadeh, H., & Imani, M. (in press). Miscibility study of chitosan/polyethylene glycol fumarate blends in dilute solutions. *Journal of Applied Polymer Science*, http://dx.doi.org/10.1002/app.37637

Hashemi Doulabi, A., Mirzadeh, H., Imani, M., Sharifi, S., Atai, M., & Mehdipour-Ataei, S. (2008). Synthesis and preparation of biodegradable and visible light crosslinkable unsaturated fumarate-based networks for biomedical applications. *Polymers for Advanced Technologies*, *19*, 1199–1208.

Hashemi Doulabi, A., Sharifi, S., Imani, M., & Mirzadeh, H. (2008). Synthesis and characterization of biodegradable, in situ forming hydrogels via direct polycondensation of poly(ethylene glycol) and fumaric acid. *Iranian Polymer Journal*, *17*, 125–133.

Hirano, S., & El-Gewely, M. R. (1996). Chitin biotechnology applications. *Biotechnology Annual Review*, *2*, 237–258.

Holland, T. A., Bodde, E. W. H., Baggett, L. S., Tabata, Y., Mikos, A. G., & Jansen, J. A. (2005). Osteochondral repair in the rabbit model utilizing bilayered, degradable oligo(poly(ethylene glycol) fumarate) hydrogel scaffolds. *Journal of Biomedical Materials Research Part A*, *75*, 156–167.

Holland, T. A., Tabata, Y., & Mikos, A. G. (2005). Dual growth factor delivery from degradable oligo(poly(ethylene glycol) fumarate) hydrogel scaffolds for cartilage tissue engineering. *Journal of Controlled Release*, *101*, 111–125.

Kim, S. K. (2011). *Chitin, chitosan, oligosaccharides and their derivatives*. New York: CRC Press, Taylor & Francis Group.

Krishna Rao, K. S. V., Ramasubba Reddy, P., Lee, Y. I., & Kim, C. (2012). Synthesis and characterization of chitosan-PEG-Ag nanocomposites for antimicrobial application. *Carbohydrate Polymers*, *87*, 920–925.

Li, P., Poon, Y. F., Li, W., Zhu, H. Y., Yeap, S. H., Cao, Y., et al. (2011). A polycationic antimicrobial and biocompatible hydrogel with microbe membrane suctioning ability. *Nature Materials*, *10*, 149–156.

Malafaya, P. B., & Reis, R. L. (2009). Bilayered chitosan-based scaffolds for osteochondral tissue engineering: Influence of hydroxyapatite on in vitro cytotoxicity and dynamic bioactivity studies in a specific double-chamber bioreactor. *Acta Biomaterialia*, *5*, 644–660.

Muzzarelli, R. A. A. (1977). *Chitin*. Oxford, UK: Pergamon.

Muzzarelli, R. A. A. (2012). Nanochitins and nanochitosans, paving the way to eco-friendly and energy-saving exploitation of marine resources. In K. Matyjaszewski, & M. Moller (Eds.), *Polymer science: A comprehensive reference* (pp. 153–164). Amsterdam: Elsevier BV.

Muzzarelli, R. A. A., Greco, F., Busilacchi, A., Sollazzo, V., & Gigante, A. (2012). Chitosan, hyaluronan and chondroitin sulfate in tissue engineering for cartilage regeneration: A review. *Carbohydrate Polymers*, *89*, 723–739.

Muzzarelli, R. A. A., Tarsi, R., Filippini, O., Giovanetti, E., Biagini, G., & Varaldo, P. E. (1990). Antimicrobial properties of *N*-carboxybutyl chitosan. *Antimicrobial Agent and Chemotherapy*, *34*, 2019–2023.

Pinto, R. J. B., Fernandes, S. C. M., Freire, C. S. R., Sadocco, P., Causio, J., Neto, C. P., et al. (2012). Antibacterial activity of optically transparent nanocomposite films based on chitosan or its derivatives and silver nanoparticles. *Carbohydrate Research*, *348*, 77–83.

Ratner, B. D. (1996). Surface properties of materials. In B. D. Ratner, A. Hoffman, F. Schoen, & J. Lemon (Eds.), *Biomaterials science: An introduction to materials in medicine* (pp. 21–25). New York: Academic Press.

Sarasam, A., & Madihally, S. V. (2005). Characterization of chitosan–polycaprolactone blends for tissue engineering applications. *Biomaterials*, *26*, 5500–5508.

Sarasam, A. R., Krishnaswamy, R. K., & Madihally, S. V. (2006). Blending chitosan with polycaprolactone: Effects on physicochemical and antibacterial properties. *Biomacromolecules*, *7*, 1131–1138.

Seyednejad, H., Imani, M., Jamieson, T., & Seifalian, A. M. (2007). Topical haemostatic agents. *British Journal of Surgery*, *95*, 1197–1225.

Sharifi, S., Kamali, M., Mohtaram, N. K., Shokrgozar, M. A., Rabiee, S. M., Atai, M., et al. (2011). Preparation, mechanical properties, and in vitro biocompatibility of novel nanocomposites based on polyhexamethylene carbonate fumarate and nanohydroxyapatite. *Polymers for Advanced Technologies*, *22*, 605–611.

Sharifi, S., Mirzadeh, H., Imani, M., Rong, Z., Jamshidi, A., Shokrgozar, M., et al. (2009). Injectable in situ forming drug delivery system based on poly([ε]-caprolactone fumarate) for tamoxifen citrate delivery: Gelation characteristics, in vitro drug release and anti-cancer evaluation. *Acta Biomaterialia*, *5*, 1966–1978.

Sharifi, S., Mirzadeh, H., Imani, M., Ziaee, F., Tajabadi, M., Jamshidi, A., et al. (2008). Synthesis, photocrosslinking characteristics, and biocompatibility evaluation of *N*-vinyl pyrrolidone/polycaprolactone fumarate biomaterials using a new proton scavenger. *Polymers for Advanced Technologies*, *19*, 1828–1838.

Shin, H., Temenoff, J. S., & Mikos, A. G. (2003). In vitro cytotoxicity of unsaturated oligo[poly(ethylene glycol) fumarate] macromers and their cross-linked hydrogels. *Biomacromolecules*, *4*, 552–560.

Solouk, A., Cousins, B. G., Mirzadeh, H., Solati-Hashtjin, M., Najarian, S., & Seifalian, A. M. (2011). Surface modification of POSSnanocomposite biomaterials using reactive oxygen plasma treatment for cardiovascular surgical implant applications. *Biotechnology and Applied Biochemistry*, *58*, 147–161.

Suggs, L. J., Payne, R. G., Yaszemski, M. J., Alemany, L. B., & Mikos, A. G. (1997). Synthesis and characterization of a block copolymer consisting of poly(propylene fumarate) and poly(ethylene glycol). *Macromolecules*, *30*, 4318–4323.

Sun, Y., Liu, Y., Li, Y., Lv, M., Li, P., Xu, H., et al. (2011). Preparation and characterization of novel curdlan/chitosan blending membranes for antibacterial applications. *Carbohydrate Polymers*, *84*, 952–959.

Suyatma, N. E., Copinet, A., Tighzert, L., & Coma, V. (2004). Mechanical and barrier properties of biodegradable films made from chitosan and poly (lactic acid) blends. *Journal of Polymers and the Environment*, *12*, 1–6.

Torres-Giner, S., Ocio, M. J., & Lagaron, J. M. (2009). Novel antimicrobial ultrathin structures of zein/chitosan blends obtained by electrospinning. *Carbohydrate Polymers*, *77*, 261–266.

Wang, Q., Dong, Z., Du, Y., & Kennedy, J. F. (2007). Controlled release of ciprofloxacin hydrochloride from chitosan/polyethylene glycol blend films. *Carbohydrate Polymers*, *69*, 336–343.

Wang, T., Zhu, X. K., Xue, X. T., & Wu, D. Y. (2012). Hydrogel sheets of chitosan, honey and gelatin as burn wound dressings. *Carbohydrate Polymers*, *88*, 75–83.

Yang, J. M., Lin, H. T., Wu, T. H., & Chen, C. C. (2003). Wettability and antibacterial assessment of chitosan containing radiation-induced graft nonwoven fabric of polypropylene-*g*-acrylic acid. *Journal of Applied Polymer Science*, *90*, 1331–1336.

Yang, J. M., Su, W. Y., Leu, T. L., & Yang, M. C. (2004). Evaluation of chitosan/PVA blended hydrogel membranes. *Journal of Membrane Science*, *236*, 39–51.

Ye, X., Kennedy, J. F., Li, B., & Xie, B. J. (2006). Condensed state structure and biocompatibility of the konjac glucomannan/chitosan blend films. *Carbohydrate Polymers*, *64*, 532–538.

Yoo, H. J., & Kim, H. D. (2008). Characteristics of waterborne polyurethane/poly(*N*-vinylpyrrolidone) composite films for wound-healing dressings. *Journal of Applied Polymer Science*, *107*, 331–338.

Zeng, M., Fang, Z., & Xu, C. (2004). Effect of compatibility on the structure of the microporous membrane prepared by selective dissolution of chitosan/synthetic polymer blend membrane. *Journal of Membrane Science*, *230*, 175–181.

Zhang, M., Li, X. H., Gong, Y. D., Zhao, N. M., & Zhang, X. F. (2002). Properties and biocompatibility of chitosan films modified by blending with PEG. *Biomaterials*, *23*, 2641–2648.

Zivanovic, S., Li, J., Davidson, P. M., & Kit, K. (2007). Physical, mechanical, and antibacterial properties of chitosan/PEO blend films. *Biomacromolecules*, *8*, 1505–1510.